

# Chapter 14

## Ultrasonic Manipulation of Single Cells

Martin Wiklund and Björn Önfelt

### Abstract

Ultrasonic manipulation has emerged as a simple and powerful tool for trapping, aggregation, and separation of cells. During the last decade, an increasing amount of applications in the microscale format has been demonstrated, of which the most important is acoustophoresis (continuous acoustic cell or particle separation). Traditionally, the technology has proven to be suitable for treatment of high-density cell and particle suspensions, where large cell and particle numbers are handled simultaneously. In this chapter, we describe how ultrasound can be combined with microfluidics and microplates for particle and cell manipulation approaching the single-cell level. We demonstrate different cell handling methods with the purpose to select, trap, aggregate, and position individual cells in microdevices based on multifrequency ultrasonic actuation, and we discuss applications of the technology involving immune cell interaction studies.

**Key words:** Ultrasonic manipulation, Acoustic trapping, Acoustophoresis, Sono-cage, Single cells

---

## 1. Introduction

### 1.1. Background

Methods for manipulating single cells date back to the early twentieth century when Barber demonstrated how to grasp a cell with suction through a hollow glass micropipette tip (1). Today, this method is still the standard technique for handling and manipulation of single cells, although it requires a skillful operator and can easily damage the cell (2). More recently, methods based on external force fields have emerged as a contactless alternative (3). Two such established techniques—negative dielectrophoresis (nDEP) (4) and laser tweezers (5)—are based on electrical and optical forces, respectively. Their main advantage is the high spatial accuracy defined by, e.g., microelectrodes or a focused laser beam, both having length scales of the order of a single cell or even smaller. Of particular interest for this chapter, however, is ultrasonic cell manipulation, sometimes

called acoustic trapping or ultrasonic standing wave (USW) manipulation (6). This technique provides a simple, powerful, and possibly more gentle tool for trapping, aggregation, or alignment of particles or cells (7), in particular in microfluidic devices (3, 8). However, in comparison to electrical or optical cell manipulation, ultrasonic manipulation is generally not associated with the high spatial accuracy needed for single-cell handling. Instead, ultrasound is known as an efficient tool for, e.g., high-throughput cell separation (“acoustophoresis”) (8) or cell aggregation in mL-volume cell suspensions (9) capable of simultaneous handling of cell numbers ranging from thousands to several millions. Nevertheless, ultrasound has recently been demonstrated to be capable of cell manipulation approaching the single-cell level (10, 11). This chapter focuses on the principles, design, and biocompatibility of devices for ultrasonic manipulation of single cells, and their use for studying immune cell interactions.

## 1.2. Principles

The principle behind ultrasonic manipulation of small, suspended particles is based on the time-averaged acoustic radiation force obtained from a nonlinear effect in the acoustic pressure field. More than a century ago, Lord Rayleigh described this nonlinear effect as the difference between the average pressure at a surface moving with the sound field and the pressure that would have existed in the fluid of the same mean density at rest (12). This simple definition was not only followed by more rigorous theoretical analyses on the force acting on suspended particles, but also many discussions about the physical interpretation of the phenomenon (13). Today, a generalized model first presented by Gor’kov in 1962 (14) is the most commonly used equation for predicting the acoustic radiation force,  $\mathbf{F}$ , in an arbitrary sound field,  $p$ , (15):

$$\mathbf{F} = -\frac{V_p \beta_f}{4} \nabla \left( f_1 p^2 - \frac{3}{2k^2} f_2 (\nabla p)^2 \right)$$

with

$$f_1 = 1 - \frac{\beta_p}{\beta_f} \quad \text{and} \quad f_2 = 2 \frac{(\rho_p - \rho_f)}{2\rho_p + \rho_f}.$$

Here,  $p$  is the acoustic pressure amplitude,  $V_p$  is the volume of the particle,  $\beta = 1/(\rho c^2)$  is the compressibility (defined by the density,  $\rho$ , and the sound speed,  $c$ ),  $k = \omega/c$  is the wave number, and  $f_1$  and  $f_2$  are the acoustic contrast factors defined by the compressibility  $\beta$  and the density  $\rho$ . The index “p” denotes “fluid” and the index “p” denotes “particle.” From the equation, we conclude that the radiation force drives suspended particles in a direction parallel with the gradient of the acoustic field and has a direction and magnitude defined by the contrast factors  $f_1$  and  $f_2$ . Obviously, steeper gradients result in

stronger forces. Now, if we aim for manipulating single cells, it should be preferable to have an acoustic field with gradients of scales approaching the size of the cell (i.e., approximately 10  $\mu\text{m}$ ). Two simple methods for creating strong gradients are available: either to focus a propagating acoustic wave or to set up a standing wave by multiple reflections in a resonating chamber. The latter method is by far the most common one (6), resulting in particles or cells driven to the pressure nodes of the USW. Once in the pressure nodes, the particles tend to aggregate into large and flat clusters oriented parallel with the reflecting walls of the chamber and with half-wavelength spacing between the clusters (in chambers with several pressure nodes). The size of these planar clusters can be further decreased by combining the standing wave with a focusing resonator geometry (16, 17). In these studies, acoustic traps were investigated with sizes of the order of a few hundred microns at frequencies up to approximately 10 MHz. Thus, this is the typical size range that defines the spatial accuracy of an acoustic tweezer aimed for single-cell handling. In other words, under these circumstances, it is very difficult to use ultrasound for selectively manipulating a single cell in a high-cell-density bulk suspension. Indeed, one solution would be to decrease the size of the acoustic field gradient by extending the acoustic frequency into the range 10–100 MHz. However, this is difficult to achieve with conventional bulk acoustic wave (BAW) technology, which is typically limited to frequencies lower than  $\sim 15$  MHz. The reason is the thin size of the piezoelectric plate when increasing the frequency (see Subheading 2.2). On the other hand, manipulation at higher frequencies (typically, up to 150 MHz) has been demonstrated by the use of surface acoustic wave (SAW) technology (18). Although SAW technology is very promising and has potential for single cell manipulation, the biocompatibility of ultrasonic manipulation at these frequencies ( $\sim 30$ –150 MHz) has to our knowledge not yet been investigated.

Thus, instead of increasing the spatial accuracy by increasing the frequency, our suggestion is to combine sub-10-MHz acoustic trapping with microfluidic control. Here, microfluidics is used to dispense individual cells into the acoustic traps. In the following sections, we describe how to design and operate an acoustic trap combining microfluidics and acoustics, with the purpose to manipulate individual cells.

---

## 2. Materials

### 2.1. Resonator Design

The traditional design of an ultrasonic resonator aimed for particle manipulation in a microfluidic device is to match the cross-section width (or height) of a fluid channel with half the acoustic wavelength,  $\lambda/2$ , (or a multiple thereof) (6). For a given channel dimension,  $L$ ,

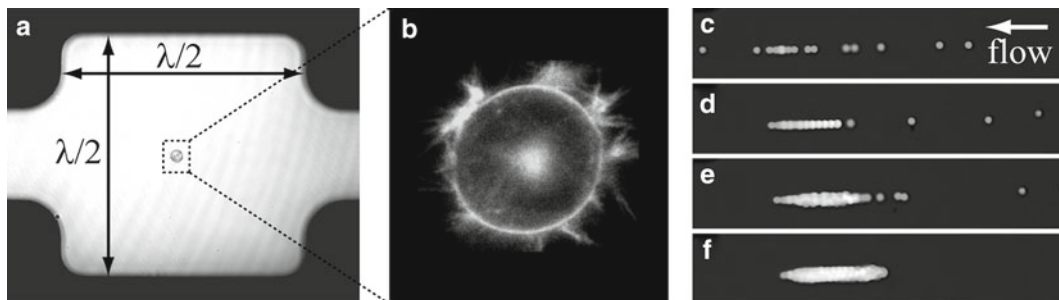


Fig. 1. (a) A single trapped human immune cell in a  $300 \times 300 \times 110\text{-}\mu\text{m}^3$  sono-cage. (b) High-resolution confocal fluorescence microscopy imaging of the same cell labeled with a membrane probe. (c–f) Selected frames from a  $\sim 1$ -min video clip demonstrating trapping and aggregation of  $10\text{-}\mu\text{m}$  beads fed into the sono-cage by the use of a continuous fluid flow. Experiment by Björn Önfelt and Otto Manneberg.

the actuation frequency is then given by the relationship  $f = c / \lambda = c / 2L$  for a single-node trap (19) or  $f = m \times c / 2L$  for a multinode trap (where  $m$  is an integer) (20). This condition gives a rough guideline of a suitable driving frequency, but in most cases further fine-tuning of the frequency needs to be performed for optimal manipulation efficiency. For single-cell three-dimensional (3-D) manipulation, the strategy is to combine orthogonal half-wave resonances with one  $f = c / 2L$  condition for each direction along the  $x$ ,  $y$ , and  $z$  axes. In practice, this is realized by introducing a rectangular cuboid compartment, called a *sono-cage*, into a microchannel, where individual cells can be trapped and retained close to the center of the cage, see Fig. 1. This compartment typically has larger dimensions than the channel cross-section area. The modes of operation of different sono-cage designs are described in Subheading 3.

In contrast to macroscaled (i.e., mm to cm scaled) ultrasonic manipulation devices (7), resonators integrated into microfluidic chips have proven to be less dependent on the outer device design, such as the dimensions of the solid structures surrounding the microfluidic channel. Macroscaled devices are often designed as multilayer resonators, where the acoustic transducer is part of the resonator (6, 19, 21). In such systems, it is very important to accurately select proper layer dimensions of both the transducer and the supporting structures to the fluid chamber. The reason for this is the coupling of resonances between different layers, which makes it a relatively complex task to predict the optimal driving frequency. Microscaled devices, however, can be actuated from almost an arbitrary coupling point with good performance, as long as the fluid channel is correctly dimensioned relative to the acoustic wavelength. One good example is a method developed by Laurell and coworkers (8), where a large transducer covering the entire bottom surface of the chip is used to excite a standing wave in the fluid channel.

Interestingly, this standing wave is typically selected to have a propagation direction perpendicular to the vibration direction of the transducer element without causing any apparent coupling problem. A related strategy uses Lamb-type plate vibrations of a glass layer in contact with the fluid chamber (20). In another example developed by us (22), a smaller (few mm wide) transducer with a coupling wedge is placed close to a corner of the chip. This method makes it possible to use several transducers operating at many different frequencies, and also to use high-resolution transillumination optical microscopy (where the latter is important for characterizing single cells). A last example mentioned here is to integrate a minimal (~1-mm wide) transducer directly in the fluid channel and use a similar design as the conventional macroscale multilayer resonator design (23). Although this method was originally designed for high-throughput trapping and separation applications (24, 25), it can be used for single-cell manipulation if it is combined with accurate microfluidic control (26).

The standing wave inside the fluid channel is built up by multiple reflections in the supporting channel walls. Thus, these walls act as acoustic mirrors. Two mirror properties need to be considered here: reflectivity and surface roughness. In acoustics, reflectivity,  $R_I$  (i.e., relative reflected intensity), is calculated from differences in acoustic impedance,  $Z$ , between the medium (fluid) and the reflector (chip material) according to  $R_I = \left[ \frac{Z_{\text{refl}} - Z_{\text{fluid}}}{Z_{\text{refl}} + Z_{\text{fluid}}} \right]^2$ . Approximate values of  $R_I$  in common chip materials with water channels are 70% for silicon, 60% for glass, 10% for PMMA, 5% for SU-8, and 4% for PDMS. Therefore, silicon and glass are the most popular materials (8), but plastics have also been employed in a few studies (27, 28). The main reason that plastics work under certain circumstances in BAW transducer systems is due to the fact that the reflectivity from any fluid or solid to air is of the order of 99.9% or higher. Thus, all energy delivered to the chip remains in the transducer—chip system including the fluid channel. Therefore, the material choice is more a question about losses and geometry than reflectivity. Losses can be quantified by the quality factor ( $Q$ ) of the resonator, which is a measure of the amplification of a vibration in the resonator.  $Q$  is also a measure of the sharpness of the resonance frequency according to  $Q = f_c / \Delta f$  (where  $f_c$  is the center frequency and  $\Delta f$  is the bandwidth). Low losses result in high- $Q$  (frequency specific) resonators while high losses cause the opposite leading to damping and heating. Typically, silicon and glass are high- $Q$  materials while plastics are low- $Q$  materials. When the device is used with optical microscopy, the damping properties of a chip holder may also influence the  $Q$  value and frequency response.

The other reflectivity property to be considered is the surface roughness of the acoustic mirrors (i.e., the channel walls). Just like in optics, the roughness of a mirror is related to the scale of the wavelength. However, ultrasonic wavelengths in water at 1–10-MHz

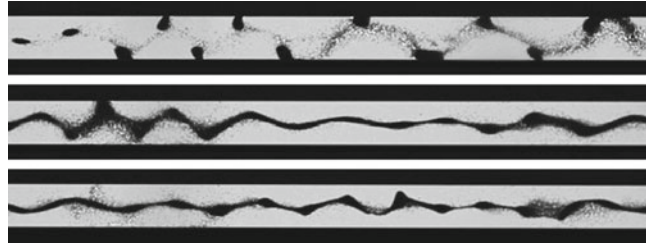


Fig. 2. Demonstration of strong mode coupling when a microfluidic channel is driven in half-wave mode, causing a wavy and striated line of focused particles. Here, the three images show the effect of changing the transducer geometry but for the same actuation frequency. Similar patterns appear when fine-tuning the actuation frequency. Experiment by Ida Iranmanesh.

frequencies are of the order of a few hundred microns. Thus, any roughness with scale 1–2 orders of magnitude lower (i.e., a few microns) is invisible to the ultrasonic wave. A good example demonstrating this is a study by Laurell and coworkers, in which a relatively rough and also asymmetric microchannel etched in glass showed a sufficiently good efficiency in manipulating suspended particles (29).

The last matter to discuss related to resonator design is the problem with unwanted mode coupling in orthogonal directions in a microchannel. For example, if the resonating direction in a rectangular cuboid compartment is along the longest side, there is no risk of any mode coupling in an orthogonal direction as long as the resonator is driven in single-node (half-wave) mode. The obvious reason is that any other direction in the rectangular cuboid then corresponds to less than a half-wave at this driving frequency. However, in acoustophoresis, the resonating direction is typically oriented across the channel width while the longest cuboid side is along the fluid channel. This means that when the half-wave condition is fulfilled across the channel width there is a significant risk of having an  $f = m \times c / 2L$  condition fulfilled along the channel at the same frequency (where  $m$  is an integer). The risk actually increases with increasing aspect ratio (length vs. width) of the channel due to the smaller (relative) frequency step when going from  $m$  to  $m + 1$  for higher values of  $m$ . A more theoretical approach to this problem is discussed in ref. 30. In practice, the effect of mode coupling appears as a nonuniform manipulation performance along the channel, often with a wavy and/or striated alignment pattern of focused particles, see Fig. 2. Strategies to avoid or circumvent this problem are discussed in Subheading 3.1.

## 2.2. Transducer Design

Most transducers used for ultrasonic manipulation of particles are based on a piezoelectric ceramic plate, often referred to as a piezo-ceramic plate, crystal, or simply a “piezo.” A common material is lead zirconate titanate (PZT), which is a ceramic compound of lead,

zirconium, and titanate. For particle manipulation purposes, hard PZT materials are preferred, such as the material “Pz-26” from Ferroperm Piezoceramics A/S, Denmark. When applying an AC voltage over the piezo, a mechanical vibration is induced capable of transmitting an ultrasonic wave away from the surface. Typically, a few volts of actuation voltage amplitude corresponds to ~1-nm displacement amplitude of the vibrating piezo surface, which is enough for generating acoustic pressure amplitudes of the order of one atmospheric pressure (atm). Typically, 1–10-atm pressure amplitudes are needed for efficient cell manipulation. This pressure range is also safe from a biocompatibility point of view (see Subheading 3.7).

A naked piezo can act as an efficient transducer itself, but it is often combined with a coupling layer and a protective housing. Most of the devices described in Subheading 3 use wedges as coupling layers for oblique acoustic coupling into the chip (22). The main purpose of a coupling layer is to increase the transmission by impedance matching, but it can also act as a protective layer between the piezo and the chip, as a heat sink, or as a spacer for minimizing near-field effects. Suitable coupling layers for transducers used on microfluidic chips are, e.g., aluminum and titanium for coupling into glass and silicon, respectively (see Note 1). It should also be mentioned that a coupling medium is needed in between the transducer and the chip to fill out all microscopic air gaps present between the two solid surfaces facing each other (see Note 2). Typically, an acoustically transparent fluid is used, such as a water-based gel, glycerol, oil, or glue. The coupling medium should be as thin as possible and assembled in such a way that no air bubble is entrapped in between the transducer and chip. A too thick layer of coupling medium will introduce unwanted losses, in particular if glue or oil is used. In terms of robustness, glue is the most popular choice of coupling medium. On the other hand, gel, glycerol, or oil is a suitable choice if a nonpermanent transducer—chip assembly procedure—is preferred.

Another vital part of a transducer is the backing layer. Traditionally, backing layers are used in medical diagnostic transducers for producing short pulses. However, for particle manipulation purposes, the conventional design is to use air-backed transducers intended for high- $Q$  continuous-wave driving mode. This implies low losses but also very-narrow-frequency bandwidths which makes it more difficult to match the transducer resonance with the resonance of the microfluidic chip. Recently, there has been some interest in designing broadband resonators/transducers for higher flexibility in particle manipulation devices (31).

### **2.3. Selection and Preparation of Cells for Ultrasonic Manipulation**

Several different cell types have been used for ultrasonic manipulation, e.g., yeast (32), plant cells (33), and many different types of mammalian cells (34). Also, various types of bacteria have been manipulated (35). For practical reasons, mostly cell lines which are

easy to grow and often quite robust have been used, but there are also examples where primary cells have been used (16, 36, 37). In ultrasonic trapping experiments, it is of particular interest to investigate cells with functions that depend on cell–cell contact. Examples of that are gap junctions formed between adjacent cells (37) trapped by ultrasound. Another example from our group is to study lymphocytes (38), which rely on cell contact and recognition by cell surface receptors to survey other cells for signs of disease (see Note 9). For example, T cells and B cells scan other cells searching for expression of disease-associated antigen, and upon stimulation of the B- or T-cell receptors these cells become activated. Natural killer (NK) cells on the other hand have the ability to directly kill virus-infected or transformed cells. This killing depends on a balance between activating and inhibitory signals mediated by cell-surface receptors on the NK cell and ligands expressed by the target cell. Thus, by using ultrasound to force NK cells and target cells together, investigations of target cell recognition mechanisms can be facilitated; see Subheading 3.5.

Primary lymphocytes can be isolated from blood through negative or positive sorting with magnetic beads or by FACS. The two latter methods have the drawback that the isolated cells are left coated with antibodies and/or magnetic beads.

Typically, the cells need to be fluorescently labeled to (1) separate different cell types from each other and (2) study cell survival or (3) the dynamics of specific proteins inside or on the surface of the cells. Separation of different cell types could be done, e.g., using dyes accumulating in the cell cytoplasm or dyes that bind to cell membranes. For the separation of live and dead cells, several different dyes are available, for example Calcein AM selectively stain the cytoplasm of living cells after hydrolysis of a acetomethyl ester. During the hydrolysis, the dye becomes charged resulting in significantly slower transport across the cell membrane. However, as cells die, the membrane becomes compromised making it possible to study cell death in real time through leakage of Calcein. There are also various dyes for selectively labeling dead cells and many of these are based on dyes leaking into the cell through the compromised plasma membrane labeling the nucleus. Thus, these dyes need to be present in the cell medium if killing is to be studied in real time. However, as several of these dyes are toxic to cells, their usefulness in long-term live-cell imaging is restricted.

For labeling specific proteins, it is possible to use fluorescently labeled antibodies or fab fragments. A restriction with antibodies is that they only label proteins on the surface of live cells and there is always a risk that the presence of the antibody can influence the interaction with other cells by blocking the protein's normal function. It is of course also possible to use molecular biology tools to make cells express proteins that are linked to, e.g., green fluorescent protein (GFP). This technique has revolutionized live-cell imaging

as it has made it possible to study the localization and dynamics of many proteins in real time. Drawbacks of using these techniques are that it often results in overexpression of the protein under investigation, raises questions about potential effects of tagging with GFP, and the fact that it is difficult to achieve expression in many types of primary cells.

---

### 3. Methods

The following methods review the work by Wiklund and coworkers at the Royal Institute of Technology on the ultrasonic handling of individual cells.

#### **3.1. Prealignment and Transport of Cells**

Alignment or focusing of cells in a microchannel is the basic mode of operation in any ultrasonic manipulation device of microfluidic format. If the purpose is to separate cells, either from a suspending medium or from other cells/particles, the term *acoustophoresis* is often used for this mode of operation. The principle is simply to vibrate a chip having a microchannel with constant (and preferably rectangular) cross section at a frequency corresponding to a half-wave across the channel width (see Subheading 2.1). Combining the cell alignment with a continuous laminar flow, this single-frequency and one-dimensional ultrasonic manipulation method is sufficient for achieving a satisfying performance. However, single-cell handling often requires lower cell concentrations and lower flow rates than normally used during high-throughput acoustophoresis. For example, in single-cell applications, it may be important to prevent cell sedimentation and to achieve a more uniform manipulation effect along the microchannel. This would lead to more uniform cell velocities in the (parabolic profiled) fluid flow, and also lower risk of unwanted interaction or attachment of cells to the channel walls. In such cases, the wavy and striated alignment pattern discussed in Subheading 2.1 (and illustrated in Fig. 2) must be eliminated or at least suppressed. A relatively simple and robust approach to solve this problem is to actuate the system with a frequency modulation scheme (39). This method is based on averaging many possible single-resonance frequencies in a microchannel by cycling linear frequency sweeps (i.e., saw-tooth modulation) over an, e.g., ~100-kHz bandwidth around a center frequency of a few MHz. The method works particularly well if the channel is long relative to the width (see Subheading 2.1) and for channels with square-shaped cross sections (i.e., with equal widths and heights). The reason for the latter is that a channel with square-shaped cross section has similar, but in practice never identical, resonance conditions in the two orthogonal directions along the width and height.

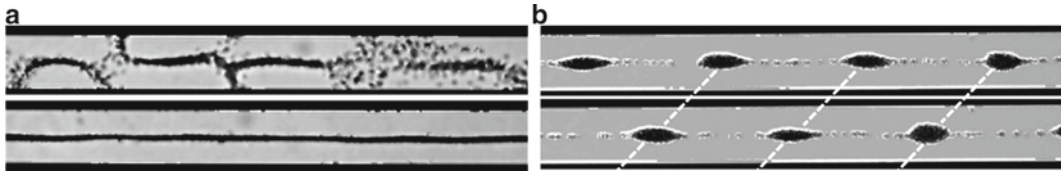


Fig. 3. Demonstration of the effect of fast (a) and slow (b) frequency-modulation actuation for uniform alignment and flow-free particle transport, respectively. (a) The upper panel shows the typical pattern of manipulated particles when the chip is driven at a single frequency (6.9 MHz). The lower panel shows the effect of cycling linear frequency sweeps at the rate 1 kHz, center frequency 6.9 MHz, and bandwidth 100 kHz. (b) The procedure in (a) is combined with cycling the frequency at the rate 0.5 Hz, center frequency 2.62 MHz, and bandwidth 40 kHz. The panels show two frames from a video clip separated 2 s in time. Experiment by Otto Manneberg.

The cycling rate, i.e., the modulation frequency, should be fast enough to ensure that the cell has no time to move to an area of significantly different force before changing to another resonant mode when changing the “instantaneous” frequency within the linear sweep (40). We have experimentally determined that 1-kHz cycling rate results in a force field corresponding to the average force fields for all single frequencies within the sweep (39). As a result, kHz-frequency-modulation actuation eliminates efficiently the effects of wavy and striated alignment patterns and makes it possible to guide cells along the same fluid streamline close to the center of the microchannel; see Fig. 3a. On the other hand, it is also possible to select a modulation frequency slow enough to ensure that cells do have time to move between different force fields at different frequencies. This is demonstrated in Fig. 3b, where cells are transported acoustically along a microchannel by the use of one fast-frequency-modulation actuation (1-kHz rate) around the center frequency 6.9 MHz (causing uniform cell alignment along the channel), and one slow-frequency-modulation actuation (0.2–0.7-Hz rate) around the center frequency 2.5 MHz (causing periodical cell aggregation and flow-free transport of cells along the channel). For particle transport by slow frequency modulation, the transport speed is controlled electronically by the modulation frequency. The investigated modulation rates are in good agreement with the theoretical cutoff rate of approx. 1 Hz calculated by Glynne-Jones (40).

### 3.2. Three-Dimensional Trapping of Cells

In Subheading 2.1, the basic principles of three-dimensional cell trapping is presented. The method utilizes an expansion chamber, termed a *sono-cage*, combined with an inlet and an outlet channel (see Fig. 1) for feeding the cage with cells or other particles (10). A slightly different sono-cage design is shown in Fig. 4, where the expansion chamber is formed by two counter-facing cylindrical segments. This sono-cage compartment measures  $300 \times 600 \times 110 \mu\text{m}^3$  (width  $\times$  length  $\times$  height), and has an inlet and outlet channel with cross-section area  $110 \times 110 \mu\text{m}^2$  (width  $\times$  height).

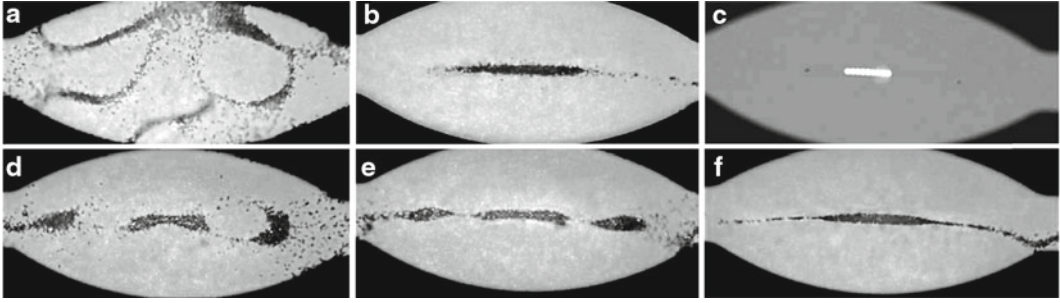


Fig. 4. Demonstration of dual-frequency actuation for three-dimensional ultrasonic manipulation: (a) 6.93 MHz/ $10 V_{p-p}$ , (b) 2.55 MHz/ $10 V_{p-p}$ , (c) 6.93 MHz/ $10 V_{p-p}$  and 2.55 MHz/ $10 V_{p-p}$ , (d) 6.93 MHz/ $10 V_{p-p}$  and 2.55 MHz/ $2 V_{p-p}$ , (e) 6.93 MHz/ $10 V_{p-p}$  and 2.55 MHz/ $6 V_{p-p}$ , (f) 6.93 MHz/ $10 V_{p-p}$  and 2.55 MHz/ $10 V_{p-p}$ . All images, except for (c), show 5- $\mu\text{m}$  beads; (c) shows 10- $\mu\text{m}$  fluorescent beads. Experiment by Otto Manneberg.

Let us now investigate how to perform 3-D trapping of particles or cells by the use of multiple-frequency ultrasonic actuation. In Fig. 4a, b, the trapping pattern of 5- $\mu\text{m}$  polystyrene beads is shown when the sono-cage is excited at 6.93 and 2.55 MHz, respectively. Here, the actuation voltage is  $10 V_{p-p}$  for both frequencies. The higher frequency is used for levitating the beads vertically from the microchannel bottom, and the lower frequency is used for focusing the beads horizontally into a compact aggregate. However, for the levitating frequency (6.93 MHz, Fig. 4a), there is an additional effect creating a complex trapping pattern within the horizontal plane. The reason for this is due to the mode coupling effect discussed in Subheading 2.1. We also note that the focusing frequency (2.55 MHz, Fig. 4b) creates an aggregate of beads on the bottom of the cage chamber. Figure 4c shows the trapping patterns of fluorescent 10- $\mu\text{m}$  beads when the sono-cage is excited with both frequencies (6.93 and 2.55 MHz) simultaneously. Here, the beads form a one-dimensional aggregate, which is trapped, levitated, and positioned close to the center of the sono-cage compartment. Thus, this dual-frequency actuation scheme makes it possible to trap and position the beads three dimensionally in a single point.

In Fig. 4d–f, the effect of gradually increasing one of the actuation voltages, while keeping the other constant, is demonstrated. Here, the 6.93-MHz transducer is excited at  $10 V_{p-p}$  constant voltage while the voltage over the 2.55-MHz transducer is increased from  $2 V_{p-p}$  (Fig. 4d) to  $6 V_{p-p}$  (Fig. 4e) and finally to  $10 V_{p-p}$  (Fig. 4f). Thus, the trapping pattern of dual-frequency actuation in Fig. 4d–f is an amplitude-weighted superposition of the individual single-frequency patterns in Fig. 4a, b. Importantly, the difference between the patterns in Fig. 4b, f is the lack of the horizontal levitation effect in Fig. 4b. Furthermore, the levitation frequency (6.93 MHz) also causes prealignment of the incoming beads, which also enhances the trapping efficiency. Finally, it should be noted that in Fig. 4c, f the transducers are operated identically

(i.e., both frequencies and same amplitudes), but with different sizes and concentrations of beads.

### 3.3. Controlling the Shape of a Trapped Cell Aggregate

An extension of the method presented in Subheading 3.2, in particular in Fig. 4d–f, is to use different amplitude ratios of two actuation frequencies for controlling the shape of a trapped cell or particle aggregate. This is illustrated in Fig. 5, where a constant actuation voltage ( $10 V_{p-p}$ ) is used for the transducer operating at the levitation frequency (6.81 MHz) while the voltage over the transducer operating at the focusing frequency (2.57 MHz) is varied from 3 to  $7 V_{p-p}$ . The effect is that the shape/dimension as well as the orientation of the aggregate can be controlled electronically; from horizontal 2-D (Fig. 5a), via compact 3-D (Fig. 5b), to vertical 2-D (Fig. 5c). This function can be of interest in studies, where it is important to control the number of neighbors in contact with each cells.

### 3.4. Selective Trapping of Cells

As mentioned in Subheading 1.1, ultrasonic traps generally do not have the spatial accuracy needed for precise and selective handling of single cells. The main reason is the  $>100\text{-}\mu\text{m}$  size of the trapping site of a typical device operating in the 1–10-MHz range. Instead, selective cell trapping can be performed if ultrasonic manipulation is combined with accurate fluid control. An example is shown in Fig. 6. Here, a large (multinode) sono-cage is combined with a prealignment channel (41). The prealignment channel can be operated in two different modes, either for single-node alignment at  $\sim 2$  MHz (half-wave resonance) or for dual-node alignment at  $\sim 4$  MHz (full-wave resonance). A third frequency ( $\sim 7$  MHz) is used for trapping cells that are injected along the central fluid streamline into the sono-cage element. As a result, 2- and 7-MHz operation leads to continuous trapping and retention of cells in the sono-cage while 4- and 7-MHz operation leads to continuous

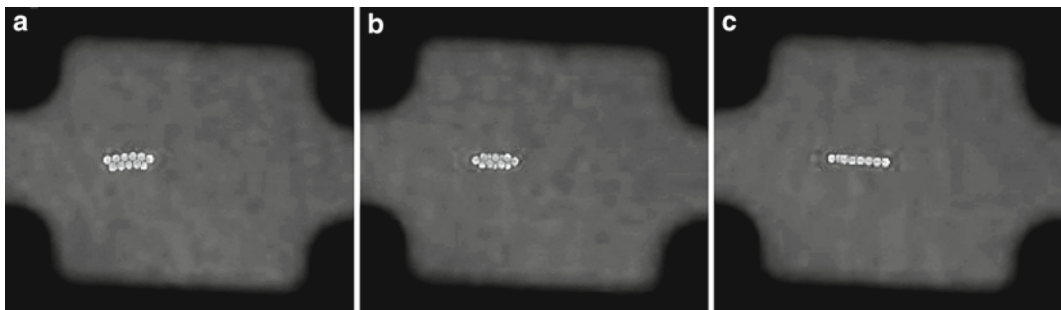


Fig. 5. Demonstration of controlling the shape and position of a bead aggregate: (a) 6.81 MHz/ $10 V_{p-p}$  and 2.57 MHz/ $3 V_{p-p}$  for a horizontal 2-D aggregate. (b) 6.81 MHz/ $10 V_{p-p}$  and 2.57 MHz/ $4 V_{p-p}$  for a 3-D aggregate. (c) 6.81 MHz/ $10 V_{p-p}$  and 2.57 MHz/ $7 V_{p-p}$  for a vertical 2-D aggregate. Experiment by Björn Önfelt and Otto Manneberg.

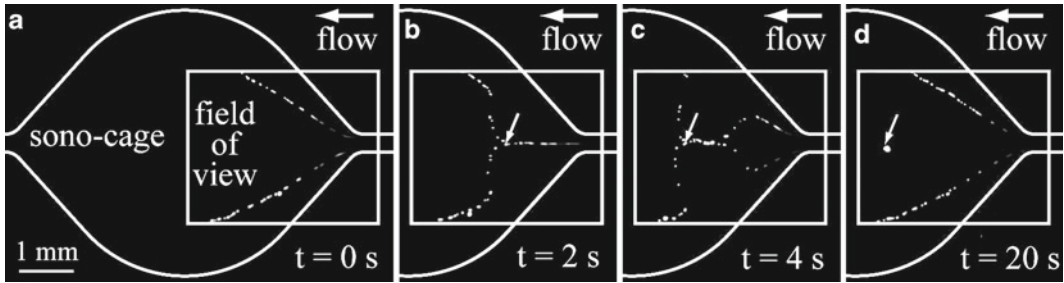


Fig. 6. Frames from a video clip demonstration of selective particle trapping and retention in a fluid flow. The large, rounded curves mark the microchannel boundaries including a 5-mm-wide sono-cage element. The rectangle marks the field of view of the microscope for monitoring the paths of 5- $\mu\text{m}$  beads. (a) 4- and 7-MHz actuation for particle bypassing. (b) 2- and 7-MHz actuation for particle injection. (c) 4- and 7-MHz actuation, back to bypassing. (d) Final trapping result. Experiment by Jessica Svennebring and Otto Manneberg.

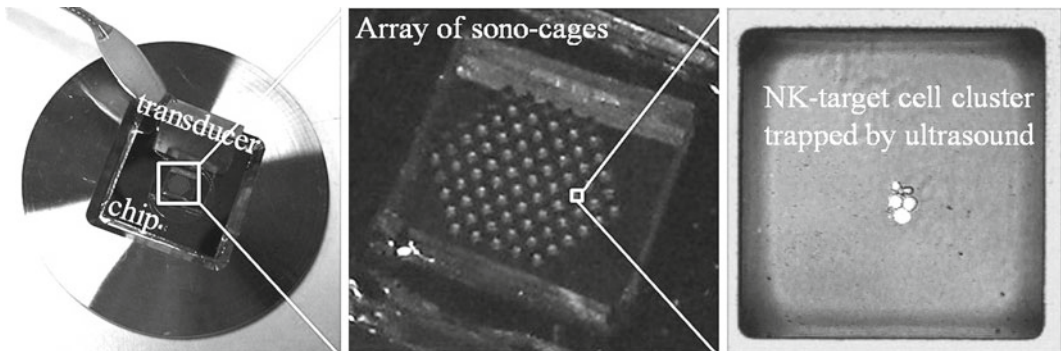


Fig. 7. An array of sono-cages integrated in a multiwell plate, and demonstration of ultrasonic merging of one natural killer (NK) cell and a few target cells. Experiments by Athanasia Christakou.

bypassing of cells through the chip without any trapping. If the actuation is switched from 4 and 7 MHz (Fig. 6a) to 2 and 7 MHz (Fig. 6b) and then back to 4 and 7 MHz (Fig. 6c), the result is injection, trapping, and positioning of a controlled number of cells into the center of the sono-cage element (Fig. 6d). The number of trapped cells can be controlled either manually given that the cell concentration is not too high or by the switching time as long as the cell concentration is constant.

### 3.5. Parallelized Merging of Cell

A microscale device for ultrasonic manipulation of cells does not necessarily have to be based on a closed microfluidic channel driven in flow-through mode. Another suitable device platform is a multiwell plate or simply a microplate. The basic sono-cage design shown in Fig. 1 (the  $300 \times 300 \times 110\text{-}\mu\text{m}^3$  rectangular cuboid) can be transferred into the microplate format by just removing the feeding channels and multiply the sono-cages into an array; see Fig. 7. Importantly, the microplate is open and easily accessible, and also free from tubings, valves, and pumps. Therefore, it is a

more simple and flexible platform, in particular for the use in long-term cellular studies.

The three-dimensional trapping method described in Subheading 3.2 utilizes two single frequencies operating simultaneously. This simple approach cannot be used in a microplate with an array of sono-cages. The reason is the complex coupling of resonances between different wells, resulting in different trapping patterns and efficiencies for different wells (11). However, this problem can be elegantly solved by implementing the frequency modulation approach described in Subheading 3.1. A similar saw-tooth modulation scheme (i.e., a few MHz center frequency, ~100-kHz bandwidth and 1-kHz sweep rate) implemented in a microplate results in merging, aggregation, and positioning of cells uniformly and simultaneously in all wells (11).

The experiments presented here utilize a simple manual pipetting method for loading cells into the wells: A droplet of cell suspension is placed on top of the plate followed by sedimentation of cells into the wells. With this method, the average number of cells per well can be controlled for the whole plate, but it is not possible to load individual cells in individual wells. However, Andersson-Svahn and coworkers have shown that individual cell loading in a similar multiwell plate as used for ultrasonic cell merging can be performed by the use of a flow cytometer (42), although these wells have significantly larger dimensions.

### **3.6. High-Resolution Imaging of Trapped Cells**

In order to make an ultrasonic manipulation device compatible with high-resolution optical microscopy, some criteria need to be considered in the design process. For microfluidic devices, the most important is to use a material with both good acoustical and good optical properties. An obvious choice is glass, which is optically transparent and has good acoustic reflectivity and low acoustic losses. Therefore, it can also function as an acoustic reflector in a standing-wave resonator. For high-resolution microscopy, the glass layer in the microchip should be of coverslip thickness for optimal image quality (when using microscope objectives that are intended to be used with coverslips). All microchips described in Subheadings 3.1–3.5 are based on bottom glass layers of thickness 200  $\mu\text{m}$ , close to the standard coverslip thickness. Given this thickness, the glass layer can be used as a quarter-wave acoustic reflector at a frequency of ~6.9 MHz for Pyrex glass. This frequency matches a half-wave chamber of 110  $\mu\text{m}$  in water, which is the choice of microchannel height in the closed devices described in Subheadings 3.1–3.4. Finally, a 1-mm top glass in Pyrex, which is an odd multiple of the quarter-wave thickness of the bottom glass, closes the resonator and provides stability to the chip (see Note 5). Thus, the vertical stack of 200- $\mu\text{m}$  bottom glass, 110- $\mu\text{m}$  silicon and water channel, and 1-mm top glass follows the traditional design of a multilayered acoustic resonator (21) and is used for

levitating the cells to the middle of the microchannel (see Subheading 3.2). In addition, this three-layer arrangement is fully transparent and therefore also compatible with any kind of transillumination microscopy technique.

### **3.7. Biocompatibility**

Ultrasonic devices utilize mechanical energy in the form of high-frequency vibrations and pressure fluctuations. This energy may cause damage to biological matters, both at the micro- and macroscale domain. One example of a destructive ultrasound application is high-intensity focused ultrasound (HIFU) used for, e.g., therapy or tissue ablation. In HIFU, heating due to absorption of acoustic energy is the main source of tissue damage. Another phenomenon that may occur in high-intensity ultrasound fields is cavitation, which can be defined as the formation and activity of microbubbles driven into violent oscillation and collapse by the acoustic field. The damage caused by cavitation is partly due to heating effects, but in particular due to mechanical shock waves and liquid jets produced when a bubble implodes. This effect is highly localized into the close vicinity of each cavitation bubble, capable of creating significant microscopic damage to a nearby surface, such as a cell membrane. Today, commercial devices based on acoustic cavitation exist, e.g., for acoustic cell lysis or acoustic membrane poration (sonoporation).

When designing a biocompatible ultrasonic manipulation device, the most important is to ensure that there is no cavitation present and that the temperature is controlled at physiologically correct levels. This strategy is the same as used in diagnostic ultrasound, where the parameters mechanical index (MI) and thermal index (TI) are used for quantifying and monitoring the potential risk of causing damage to tissue or cells as a consequence of cavitation and heating, respectively. In an ultrasonic manipulation device, the temperature can be handled in two different ways. One method is to integrate a cooling system close to the active fluid chamber, e.g., by the use of a cooling water loop or a Peltier cooler. This method is suitable for applications requiring significant powers, such as high-throughput acoustophoresis. Another method is to take advantage of the heat generated by the acoustic actuation and use the temperature increase in a temperature regulation system (43). This method is suitable for medium-power applications, where the acoustic heating corresponds to 1–10°C temperature increases. The latter method can then be combined with additional external heating, e.g., by using a heatable microscope frame as a chip holder. In this way, the temperature can be kept at a constant level (e.g., at 37°C) independently on the magnitude of the acoustic field and for long times (hours to days) (11).

While the temperature is relatively straightforward to monitor and control in an ultrasonic manipulation device, the risk of causing cavitation is unfortunately not. Instead, care must be taken not to

use acoustic pressure amplitudes close to the cavitation threshold. This threshold is dependent on many parameters, such as the frequency, type of medium, and actuation mode. As a guideline, Bazou and coworkers have measured the cavitation threshold in a typical ultrasonic manipulation device operating at 1.5 MHz to be 2 MPa (pressure amplitude) (44). This measurement was based on detecting white noise characteristic for cavitation activity by the use of a spectrum analyzer. This threshold can be compared with the typical pressure amplitudes used for efficient particle manipulation, which are in the range 0.1–1 MPa.

If the temperature and CO<sub>2</sub> levels are controlled in a similar way as in a standard cell culture system (typically, at 37°C and 5% CO<sub>2</sub>) and if the acoustic pressure amplitude is significantly lower than the cavitation threshold, cells trapped in an ultrasonic manipulation device can be kept viable with retained cellular functions during extended periods in time. In microfluidic devices, additional parameters need to be controlled, such as the biocompatibility of the different chip materials and their surfaces facing the cell sample, as well as potential shear stress from fluid flows. One of the first cell viability studies performed in a microfluidic device designed for ultrasonic manipulation demonstrated that COS-7 cells acoustically retained in a microchannel at 0.85 MPa for 75 min showed no deviation from normal growth rates when they were returned to the incubator after the ultrasound exposure (45). A more recent study showed that human immune cells were kept viable over 3 days of continuous ultrasound exposure at similar amplitudes (11). In this study, cell proliferation was observed during the exposure. It should be noted, however, that in all these studies cells were trapped and retained in the pressure nodes of an ultrasonic standing wave. Several studies suggest that ultrasonic standing waves are less damaging or stressful for cells than propagating ultrasonic waves (33, 46, 47). One reason could be that pressure fluctuations are more stressful for cells than velocity vibrations. In a pressure node, the pressure fluctuations have a minimum while the velocity vibrations have a maximum. Furthermore, cavitation is more likely to appear in the pressure antinodes than in the pressure nodes if the pressure amplitude is close to the cavitation threshold. Therefore, the acoustic radiation force in an ultrasonic manipulation system actually provides a protective effect on the cells (46).

---

## 4. Notes

1. Aluminum is a suitable coupling layer for a PZT transducer aimed for transmitting a wave into a chip made of glass. The reason is that the acoustic impedance of aluminum is in between

the impedance of PZT and glass. For silicon chips, titanium is a suitable coupling layer for the same reason.

2. The layer of liquid coupling medium between the transducer and chip should be as thin as possible and the surfaces should be parallel. The conductive adhesive gel “Tensive” from Parker Laboratories works very well for acoustic coupling and is easily removed with water. Microscope immersion oil works well as coupling medium if it is combined with a holder pressing the transducer against the chip. Since immersion oil is not an adhesive, nor evaporate, it can be used in applications, where the transducer needs to be repositioned during an experiment.
3. Plasma bonding is a suitable method to attach the PDMS frame on the multiwell chip to avoid sample leakage out to the transducer area. A glass lid placed over the frame prevents evaporation. The PDMS frame allows gas exchange between the cell sample in the chip and the environmental chamber, which is important for the long-term biocompatibility of the device.
4. Acetone efficiently dissolves beads that have adhered inside the microchannel. Ethanol followed by water and finally air should be used for washing a chip after a cell experiment.
5. For high-resolution imaging inside a closed microfluidic channel, coverslip glass with thickness  $\sim 0.2$  mm is suitable as bottom glass of the chip. The other chip layers should be 0.5–1 mm thick to retain stability and robustness of the device. When imaging cells suspended in a microchannel, a water-immersion objective is the best choice. For adherent cells on the bottom of the channel, oil immersion is the best choice.
6. When performing high-resolution imaging over large areas (several mm) based on multiple images, it is important to assemble the chip perfectly parallel with the microscope stage. If available, it is also possible to use automatic focusing.
7. As a cell model, an erythrocyte-mimicking phantom (Orgasol, 5- $\mu\text{m}$  polyamide beads) from Danish Phantom Design is a suitable and inexpensive choice. Polyamide as well as polystyrene beads have acoustic properties relatively similar to cells and respond similarly to the acoustic radiation force.
8. A temperature-controlled system is not only good for the biocompatibility, but also for stabilizing the resonance condition. Since the acoustic wavelength is dependent on the temperature, the manipulation performance may change if the temperature is drifting.
9. Several types of Immune cells are particularly suitable to study with the ultrasonic manipulation technique. One reason is that immune cells grow and function in suspension. Furthermore, immune cells, in particular lymphocytes, have functions that are dependent on cell–cell interactions. Such interactions can be induced by the ultrasonic manipulation technique.

## Acknowledgments

The authors thank former and present members of the Ultrasonic manipulation group, Department of Applied Physics, Royal Institute of Technology, Stockholm: Athanasia Christakou, Thomas Frisk, Hans Hertz, Ida Iranmanesh, Linda Johansson, Otto Manneberg, Mathias Ohlin, Jessica Svennebring, and Bruno Vanherberghen for contribution with results and proofreading.

## References

1. Barber, M. A. (1904) A new method of isolating microorganisms. *J Kansas Med Soc* 4, 489–494.
2. Fleming, S. D. and King, R. S. (2003) *Micromanipulation in Assisted Conception*. Cambridge University Press, Cambridge.
3. Nilsson, J., Evander, M., Hammarström, B. and Laurell, T. (2009) Review of cell and particle trapping in microfluidic systems. *Anal Chim Acta* 649, 141–157.
4. Duschl, C., Geggier, P., Jäger, M., Stelzle, M., Müller, T., Schnelle, T. and Fuhr, G. R. (2004) Versatile chip-based tools for the controlled manipulation of microparticles in biology using high frequency electromagnetic fields. In: Andersson, H. and van der Berg, A. Ed. *Lab-on-Chips for Cellomics. Micro and Nanotechnologies for Life Science*. Kluwer Academic Publishers, Dordrecht, The Netherlands.
5. Sott, K., Eriksson, E., Petelenz, E. and Goksör, M. (2008) Optical systems for single cell analyses. *Expert Opin Drug Discov* 3, 1323–1344.
6. Gröschl, M. (1998) Ultrasonic separation of suspended particles – Part I: Fundamentals. *Acustica Acta Acustica* 84, 432–447.
7. Gröschl, M., Burger, W., Handl, B., Doblhoff-Dier, O., Gaida, T. and Schmatz, C. (1998) Ultrasonic separation of suspended particles – Part III: Application in biotechnology. *Acustica Acta Acustica* 84, 815–822.
8. Laurell, T., Petersson, F. and Nilsson, A. (2007) Chip integrated strategies for acoustic separation and manipulation of cells and particles. *Chem Soc Rev* 36, 492–506.
9. Coakley, W. T., Hawkes, J. J., Sobanski, M. A., Cousins, C. M. and Spengler, J. (2000) Analytical scale ultrasonic standing wave manipulation of cells and microparticles. *Ultrasonics* 38, 638–641.
10. Manneberg, O., Vanherberghen, B., Svennebring, J., Hertz, H. M., Önfelt, B. and Wiklund, M. (2008) A three-dimensional ultrasonic cage for characterization of individual cells. *Appl Phys Lett* 93, 063901 (3 pp).
11. Vanherberghen, B., Manneberg, O., Christakou, A., Frisk, T., Ohlin, M., Hertz, H. M., Önfelt, B. and Wiklund, M. (2010) Ultrasound-controlled cell aggregation in a multi-well chip. *Lab Chip* 10, 2727–2732.
12. Lord Rayleigh (1905) On the momentum and pressure of gaseous vibrations, and on the connexion with virial theorem. *Philos Mag* 10, 364–374.
13. Beyer, R. T. (1978) Radiation pressure – the history of a mislabeled tensor. *J. Acoust. Soc. Am.* 63, 1025–1030.
14. Gor'kov, L. P. (1962) On the forces acting on a small particle in an acoustical field in an ideal fluid. *Sov Phys Dokl* 6 773–775.
15. O. Manneberg, Ph.D Thesis, Royal Institute of Technology, Stockholm, 2009.
16. Hertz, H. M. (1995) Standing-wave acoustic trap for noninvasive positioning of microparticles. *J Appl Phys* 78, 4845–4849.
17. Wiklund, M., Nilsson, S. and Hertz, H. M. (2001) Ultrasonic trapping in capillaries for trace-amount biomedical analysis. *J Appl Phys* 90, 421–426.
18. Wang, Z. and Zhe, J. (2011) Recent advances in particle and droplet manipulation for lab-on-a-chip devices based on surface acoustic waves. *Lab Chip*, in press, DOI: 10.1039/c0lc00527d.
19. Hawkes, J. J., Coakley, W. T., Gröschl, M., Benes, E., Armstrong, S., Tasker, P. J. and Nowotny, H. (2002) Single half-wavelength ultrasonic particle filter: Predictions of the transfer matrix multilayer resonator model and experimental filtration results. *J Acoust Soc Am* 111, 1259–1266.
20. Haake, A. and Dual, J. (2005) Contactless micromanipulation of small particles by an ultrasound field excited by a vibrating body. *J Acoust Soc Am* 117, 2752–2760.

21. Hill, M., Townsend, R. J. and Harris, N. R. (2008) Modelling for the robust design of layered resonators for ultrasonic particle manipulation. *Ultrasonics* 48, 521–528.
22. Manneberg, O., Svennebring, J., Hertz, H. M. and Wiklund, M. (2008) Wedge transducer design for two-dimensional ultrasonic manipulation in a microfluidic chip. *J Micromech Microeng* 18, 095025 (9 pp).
23. Lilliehorn, T., Simu, U., Nilsson, M., Almqvist, M., Stepinski, T., Laurell, T., Nilsson, J. and Johansson, S. (2005) Trapping of microparticles in the near-field of an ultrasonic transducer. *Ultrasonics* 43, 293–303.
24. Evander, M., Johansson, L., Lilliehorn, T., Piskur, J., Lindvall, M., Johansson, S., Almqvist, M., Laurell, T. and Nilsson, J. (2007) Noninvasive acoustic cell trapping in a microfluidic perfusion system for online bioassays. *Anal Chem* 79, 2984–2991.
25. Norris J.V., Evander M., Horsman-Hall K.M., Nilsson J., Laurell T. and Landers J.P. (2009) Acoustic differential extraction for forensic analysis of sexual assault evidence. *Anal Chem* 81, 6089–6095.
26. Johansson, L., Nikolajeff, F., Johansson, S. and Thorslund, S. (2009) On-chip fluorescence-activated cell sorting by an integrated miniaturized ultrasonic transducer. *Anal Chem* 81, 5188–5196.
27. Wiklund, M., Toivonen, J., Tirri, M., Hänninen, P. and Hertz, H. M. (2004) Ultrasonic enrichment of microspheres for ultrasensitive biomedical analysis in confocal laser-scanning fluorescence detection. *J Appl Phys* 96, 1242–1248.
28. González, I., Fernández, L. J., Gómez, T. E., Berganzo, J., Soto, J. L. and Carrato, A. (2010) A polymeric chip for micromanipulation and particle sorting by ultrasounds based on a multilayer configuration. *Sens Act B* 144, 310–317.
29. Evander, M., Lenshof, A., Laurell, T. and Nilsson, J. (2008) Acoustophoresis in wet-etched glass chips. *Anal Chem* 80, 5178–5185.
30. Barnkob, R., Augustsson, P., Laurell, T. and Bruus, H. (2010) Measuring the local pressure amplitude in microchannel acoustophoresis. *Lab Chip* 10, 563–570.
31. Ohlin, M., Frisk, T., Önfelt, B. and Wiklund, M. (2010) Frequency-shift-keying actuation with a damped transducer for ultrasonic particle aggregation in a multi-well chip. *Proc. of USWNet 2010 Conference, Groningen, The Netherlands*, 14–15.
32. Hawkes, J. J. and Coakley, W. T. (1996) A continuous flow ultrasonic cell-filtering method. *Enzyme Microbial Technol* 19, 57–62.
33. Böhm, H., Anthony, P., Davey M.R., Briarty, L.G., Power, J.B., Lowe, K. C., Benes, E. and Gröschl, M. (2000) Viability of plant cell suspensions exposed to homogeneous ultrasonic fields of different energy density and wave type. *Ultrasonics* 38, 629–632.
34. Shirgaonkar, I. Z., Lanthier, S. and Kamen, A. (2004) Acoustic cell filter: a proven cell retention technology for perfusion of animal cell cultures. *Biotechnol Adv* 22, 433–444.
35. Miles, C. A., Morley, M. J., Hudson, W. R. and Mackey, B. M. (1995) Principles of separating micro-organisms from suspensions using ultrasound. *J Appl Bacteriol* 78, 47–54.
36. Cousins, C. M., Holownia, P., Hawkes, J. J., Limaye, M. S., Price, C. P., Keay, P. J. and Coakley, W. T. (2000) Plasma preparation from whole blood using ultrasound. *Ultrasound Med Biol* 26, 881–888.
37. Bazou, D., Douthwaite, G. P., Khan, I. M., Archer, C. W., Ralphs, J. R. and Coakley, W. T. (2006) Gap junctional intercellular communication and cytoskeletal organization in chondrocytes in suspension in an ultrasound trap. *Mol Memb Biol* 23, 195–205.
38. Guldevall, K., Vanherberghen, B., Frisk, T., Hurtig, J., Christakou, A. E., Manneberg, O., Lindström, S., Andersson-Svahn, H., Wiklund, M. and Önfelt, B. (2010) Imaging Immune Surveillance of Individual Natural Killer Cells Confined in Microwell Arrays. *PLoS One* 10, e15453 (12 pp).
39. Manneberg, O., Vanherberghen, B., Önfelt, B. and Wiklund, M. (2009) Flow-free transport of cells in microchannels by frequency-modulated ultrasound. *Lab Chip* 9, 833–837.
40. Glynne-Jones, P., Boltryk, J. R., Harris, N. R., Cranny, A. W. J. and Hill, M. (2010) Mode-switching: A new technique for electronically varying the agglomeration position in an acoustic particle manipulator. *Ultrasonics* 50, 68–75.
41. Svennebring, J., Manneberg, O., Skafte-Pedersen, P., Bruus, H. and Wiklund, M. (2009) Selective bioparticle retention and characterization in a chip-integrated confocal ultrasonic cavity. *Biotech Bioeng* 103, 323–328.
42. Lindström, S., Larsson, R. and Andersson-Svahn, H. (2008) Towards high-throughput single cell/clone cultivation and analysis. *Electrophor* 29, 1219–1227.
43. Svennebring, J., Manneberg, O. and Wiklund, M. (2007) Temperature regulation during ultrasonic manipulation for long-term cell handling in a microfluidic chip. *J Micromech Microeng* 17, 2469–2474.
44. Bazou, D., Kuznetsova, L. A. and Coakley, W. T. (2005) Physical environment of 2-D animal cell aggregates formed in a short pathlength

- ultrasound standing wave trap. *Ultrasound Med Biol* 31, 423–430.
45. Hultström, J., Manneberg, O., Dopf, K., Hertz, H. M. and Wiklund, M. (2007) Proliferation and viability of adherent cells manipulated by standing-wave ultrasound in a microfluidic chip, *Ultrasound Med Biol* 33, 145–151.
  46. Nyborg, W. (2001) Biological effects of ultrasound: Development of safety guidelines. Part II: General review. *Ultrasound Med Biol* 27, 301–333.
  47. Chisti, Y. (2003) Sonobioreactors: using ultrasound for enhanced microbial productivity. *Trend Biotechnol* 21, 89–93.